ELSEVIER

Contents lists available at ScienceDirect

Ceramics International

journal homepage: www.elsevier.com/locate/ceramint





Assessment of recycling use of GFRP powder as replacement of fly ash in geopolymer paste and concrete at ambient and high temperatures

Jun Wang^{a,*}, Chuji Zheng^a, Liwu Mo^a, Hota GangaRao^b, Ruifeng Liang^b

- a College of Civil Engineering, Nanjing Tech University, Nanjing, 211816, PR China
- ^b Department of Civil and Environmental Engineering, West Virginia University, WV, USA

ARTICLE INFO

Keywords:
Glass fiber reinforced polymer powder
Fly ash
Geopolymer
Physico-mechanical properties
High temperature

ABSTRACT

Environmental issues caused by glass fiber reinforced polymer (GFRP) waste have attracted much attention. The development of cost-effective recycling and reuse methods for GFRP composite wastes is therefore essential. In this study, the formulation of the GFRP waste powder replacement was set at 20-40 wt%. The geopolymer was formed by mixing GFRP powder, fly ash (FA), steel slag (SS) and ordinary Portland cement (OPC) with a sodiumbased alkali activator. The effects of GFRP powder content, activator concentration, liquid to solid (L/S) ratio, and activator solution modulus on the physico-mechanical properties of geopolymer mixtures were identified. Based on the 28-day compressive strength, the optimal combination of the geopolymer mixture was determined to be 30 wt% GFRP powder content, an activator concentration of 85%, L/S of 0.65, and an activator solution modulus of 1.3. The ratios of compressive strength to flexural strength of the GFRP powder/FA-based geopolymers were considerably lower than those of the FA/steel slag-based geopolymers, which indicates that the incorporation of GFRP powder improved the geopolymer brittleness. The incorporation of 30% GFRP powder in geopolymer concrete to replace FA can enhance the compressive and flexural strengths of geopolymer concrete by 28%. After exposure to 600 °C, the flexural strength loss for geopolymer concretes containing 30 wt% GFRP powder was less than that of specimens without GFRP powder. After exposure to 900 °C, the compressive strength and flexural strength losses of geopolymer concretes containing 30 wt% GFRP powder were similar to those of specimens without GFRP powder. The developed GFRP powder/FA-based geopolymers exhibited comparable or superior physico-mechanical properties to those of the FA-based geopolymers, and thus offer a high application potential as building construction material.

1. Introduction

Glass fiber reinforced polymer (GFRP) composites have been extensively applied in automotive, aerospace, marine, infrastructure, and power generation engineering. Most GFRP composite structural products are made of a thermosetting resin matrix because these compositions are strong and characterized by very good fatigue strength [1–3]. However, thermoset-based composites are difficult to recycle and cannot be re-melted or remolded as thermoplastics owing to the cross-linked thermoset polymer matrix [4], which places high pressure on the environment. The development of effective recycling and reuse methods for GFRP composite wastes is therefore essential. The FRP composite waste recycling techniques mainly include mechanical, thermal, and chemical methods [5]. However, these approaches are limited by a variety of factors, including recycled fiber deterioration,

high energy consumption, high cost, long cycle time, and the release of highly toxic gases [6].

Geopolymerization is a process in which the reactive ingredients of aluminosilicate raw materials are converted into gel production. Geopolymers have been developed as an alternative to Portland cement to reduce CO₂ emissions, and offer an effective strategy to reuse waste industry by-products [7]. Any raw materials that are rich in reactive Si and Al can be used for synthesizing geopolymers, in which the Si–Al source materials are dissolved by an alkaline activator to form three-dimensional amorphous gels [8]. The commonly used aluminosilicate materials available for producing geopolymers including fly ash (FA), ground granulated blast furnace slag (GGBS), steel slag (SS), and metakaolin (MK) [9]. Because glass fibers are silica-based (~50%–60% SiO₂) and contain a host of other oxides (e.g., Al₂O₃, CaO, MgO) [10], the application of GFRP waste powder as a geopolymer precursor is

^{*} Corresponding author. College of Civil Engineering, Nanjng Tech University, Nanjing, 211816, China. *E-mail address:* wangjun3312@njtech.edu.cn (J. Wang).

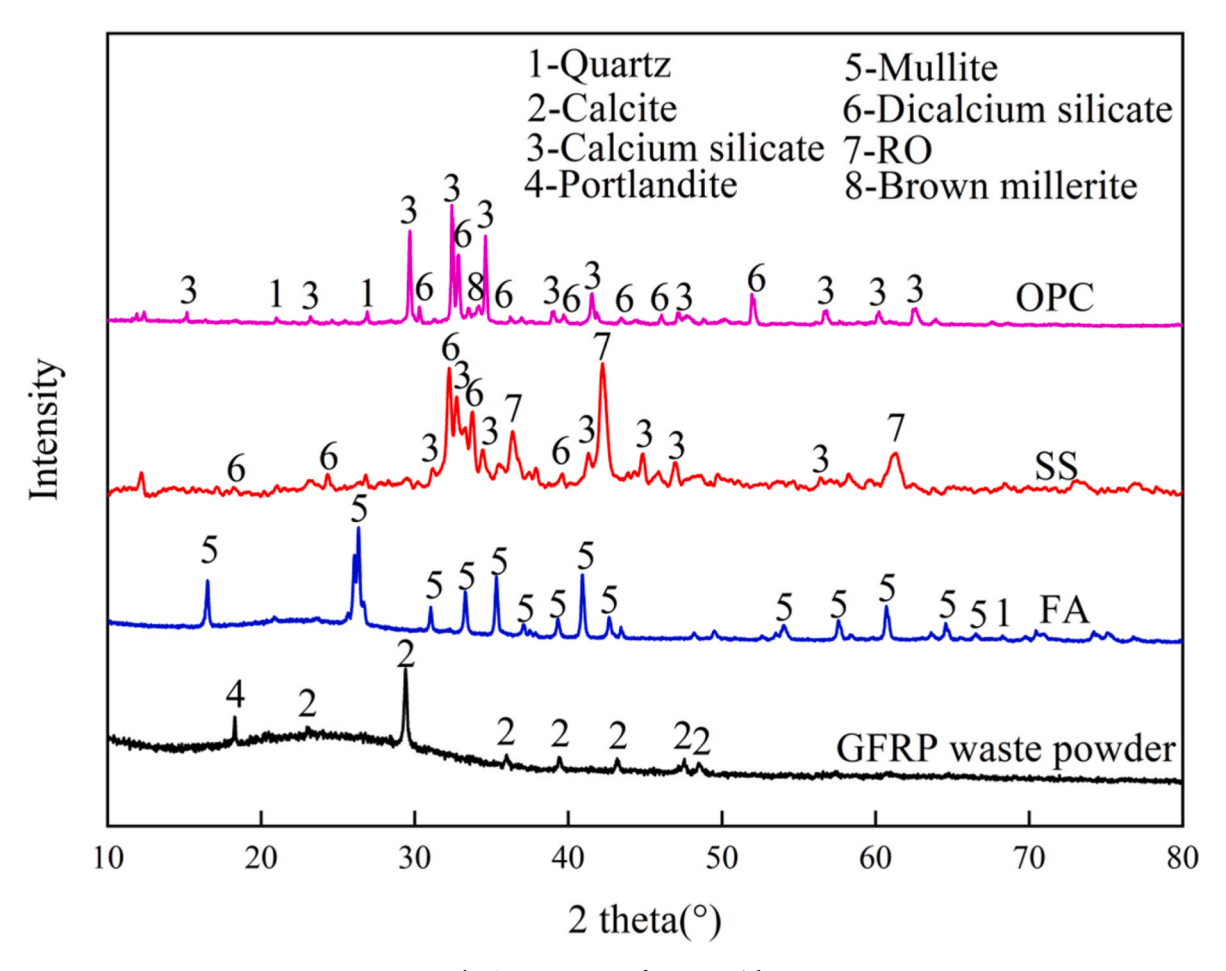


Fig. 1. XRD pattern of raw materials.

expected to be an economical and environmentally friendly strategy.

Although GFRP powder-based geopolymers have not been reported in the literature, the use of recycled glass powder (GP) or ground glass fiber (GGF) as a precursor for geopolymer manufacturing is a popular research topic because GP or GGF can be used to supply reactive silica [11,12]. Rashidian-Dezfouli and Rangaraju [13,14] studied the alkali-silica reaction (ASR) of aggregate in GGF-based geopolymer mortars and the durability of GP- and GGF-based geopolymers in sodium sulfate solution. The GGF-based geopolymer mixtures exhibited a better resistance against the ASR-related expansion compared with the ordinary Portland cement (OPC) mixture [13]. Moreover, the presence of sulfate has been shown to have an insignificant effect on the mechanical properties of GGF based geopolymers, whereas GP-based specimens are unstable in sodium sulfate solution [14]. Taveri et al. [15] reported that for silica-to-alumina ratios of 2.7-5.0 and NaOH solution molarities of 10-13 M, the highest flexure strength of GP-based geopolymer mixtures was obtained using a silica-to-alumina ratio of 3.3 and NaOH solution molarity of 13 M. The workability characteristics of GP-based geopolymer concrete can be improved by increasing the GP proportion due to its lower specific surface area, lower water absorption capacity, smooth texture, and filling ability. The partial replacement of 20%–30% GP with other aluminosilicate source materials (e.g., FA, GGBS, MK) in the geopolymer binder preparation process has been shown to enhance the geopolymer compressive strength [16]. Dadsetan et al. [17] showed that the GP has a higher silica solubility than MK, and that the dissolution rate is highly affected by the impurities of these materials. Si et al. [18] reported that a denser gel phase formed in MK-based geopolymer mixtures containing 5-10% GP, and that GP additions reduce the water loss rate of geopolymer mixtures under drying conditions, leading to reduced early-age drying shrinkage.

Geopolymers mixed with a small amount of epoxy resin can improve the geopolymeric mechanical performance. Major efforts have been made in polymer mix design using different organic resins [19,20]. Ferone et al. [21] produced organic-inorganic materials following a synthetic approach based on the co-reticulation of a MK-based geopolymer matrix and epoxy-based resin. These MK-based geopolymers with 20% epoxy resin exhibited good and homogeneous dispersion, and significantly improved the compressive strength and toughness with respect to neat geopolymers. Zhang [22] synthesized alkali-activated MK-based geopolymer mixtures with 10%, 20%, and 30% epoxy resin. Their experimental results indicated that the addition of epoxy resin to geopolymers lowered the 3-day compressive strength but increased the 28-day compressive strength of the samples because the epoxy resin extended the curing time, thus resulting in complete internal condensation stabilization. Wang et al. [23] incorporated epoxy resin into MK-based geopolymers to optimize the pore structure and reduce the pore diameter. Their experimental results indicated that the pore size distribution shifted to smaller regions when the epoxy resin content was less than 4 wt%. Colangelo et al. [24] incorporated expanded polystyrene in MK-based geopolymers as an insulating aggregate to develop lightweight thermally insulated geopolymer concrete, and modified the matrix by the addition of epoxy resin. These organic-inorganic composites showed superior properties compared with OPC-based materials, with higher strength and lower thermal conductivity. Roviello et al. [25] reported that the compressive strength of FA-based geopolymers increased by 18% and 62% upon the addition of 10% and 20% epoxy, respectively, and the microstructure analysis indicated strong interactions between the organic resin and matrix. They recommend the use of FA-based epoxy-geopolymers rather than the more expensive MK-based geopolymers.

Table 1Chemical composition of raw materials (% by mass).

Oxide	GFRP powder	Fly ash (FA)	Steel slag (SS)	OPC
SiO ₂	33.71	52.41	31.02	19.41
Al_2O_3	10.62	28.11	7.98	4.74
CaO	20.57	3.27	28.42	64.01
MgO	3.45	0.77	4.34	2.34
Fe_2O_3	0.63	4.94	23.02	2.95
SO_3	0.98	2.13	0.77	2.59
K ₂ O	0.32	2.50	0.21	0.65
Na ₂ O	0.21	0.76	0.64	-
TiO_2	0.51	1.20	0.49	_
LOI	28.12	2.8	2.13	2.82
Total	99.12	98.89	99.02	99.63

Note: Loss of ignition (LOI)-calculated through weight after materials firing.

Table 2Particle size distribution of raw materials.

Materials	d ₁₀ (μm)	d ₅₀ (μm)	d ₉₀ (μm)
FA	1.414	10.594	25.357
GFRP powder	1.583	13.506	37.841
SS	1.714	11.448	38.287
OPC	2.010	12.698	49.401

Table 3
Factors and test parameters.

Level	Factor							
	A: activator concentration (%)	B: L/ S	C: modulus of the activator solution	D: Content of GFRP powder				
1	70	0.65	1.2	20%				
2	80	0.75	1.3	30%				
3	85	0.85	1.4	40%				

Geopolymers are generally regarded as materials with good thermalphysical-mechanical properties after exposure to high temperatures due to their ceramic-like microstructures [26]. The addition of GP can improve the fire-resistance of FA-based geopolymer pastes because the geopolymer pore system is filled upon GP melting, which enhances the geopolymer gel integrity [27]. The addition of organic polymer (up to 25 wt%) in a MK-based geopolymeric matrix can improve the mechanical properties of geopolymers. However, such high organic polymer concentrations may reduce the fire resistance of the geopolymeric materials [28,29]. Roviello et al. [29] developed two kinds of innovative epoxy resins containing melamine derivatives, in which the presence of azacyclic rings ensured the high thermal stability of the epoxy-MK matrix. Zhang et al. [30] stated that the thermal decomposition of resin occurred in MK/GGBS/polyvinyl acetate-based geopolymer composites exposed to temperatures of 450-850 °C. Thermoset resin is usually unstable at temperatures above 300-400 °C [31]. However, the thermal stability of GFRP powder-based geopolymers remains unknown.

The main objective of this study is to investigate the feasibility of using GFRP powder as a partial FA replacement to produce geopolymer materials. Experiments following the orthogonal design method were performed to determine the effects of GFRP powder content, activator concentration, liquid to solid ratio (L/S), and activator solution modulus on the workability and compressive strengths of GFRP powder/FA-based geopolymer mixtures. The mixture design of the geopolymer concrete was conducted based on the proportion of geopolymer paste with the highest compressive strength, in which the effects of sand-to-aggregate ratio (s/a) and aggregate to binder ratio (a/b) were taken into account. The mechanical properties of geopolymer concrete were explored after exposure to high temperatures (300, 600, and 900 °C). X-ray diffraction (XRD), Fourier transform infrared (FTIR) spectroscopy, and scanning electron microscopy (SEM) coupled with energy-dispersive X-

Ray spectroscopy (EDS) tests were performed to investigate the microstructural characteristics of the geopolymer paste and geopolymer concrete specimens.

2. Materials and experimental program

2.1. Material characterization

Class F FA was used as the main aluminosilicate source material in the geopolymer mixtures with precursor weight percentages of 40%, 50%, and 60%. Class F FA is generally derived from bituminous and anthracite coals with a CaO content of less than 18% [32]. The main crystallinities of Class F FA determined by XRD are mullite and quartz (Fig. 1). Class F FA is considered to be more suitable for synthesizing geopolymers than Class C FA, which is produced from lignite and subbituminous coals with a CaO content of more than 18% [33]. The GFRP powder was provided by composite pultrusion manufacturer, in which the volume percent of E glass fiber and unsaturated polyester resin were 72% and 28%, respectively. The excessive additive of polymer resin may decrease the mechanical performance of geopolymers [19,20]. GFRP powder was added as an FA replacement at weight percentages of 20%, 30%, and 40%. Hence, the content of polymer resin in precursor was less than 10 wt%. The main crystallinities of the GFRP powder determined by XRD are calcite and portlandite, (Fig. 1). The bulk densities of FA and GFR powder are 1160 and 525 kg/m³, respectively. SS was added in the geopolymer mixtures at a precursor weight percentage of 10%. The main phases in SS include C_3S , β - C_2S , γ - C_2S , CaO-FeO-MnO-MgO solid solution (Fig. 1) [34,35]. The conversion of β-C₂S to γ-C₂S during cooling resulted in a slight increase in volume and made the material effectively self-pulverizing. The presence of C₃S and C₂S provides some weak cementitious properties for SS, thus increasing its basicity [36]. Guo and Pan [37] reported that the incorporation of proper content of SS had significant toughening and strengthening effects on the FA-based geopolymers, because the overall microstructure of geopolymer became denser. When the content of SS exceeds 10%, the 28-day compressive strength of the FA/SS geopolymer pastes gradually decreases due to the low activity of SS and the carbonization of unreacted free CaO in SS with the increase in age. OPC was also added in the geopolymer mixtures at a precursor weight percentage of 10%. OPC can be used as an additive to improve the early behavior of the geopolymer mixture under room temperature curing. The incorporation of OPC contributes to promote the full dissolution of silicaalumina raw materials in alkaline environment, thus improving the degree of geopolymerization. Huo et al. [38] stated that the FA-based geopolymers had the highest 28-day compressive strength when OPC content was 10% of the total cementitious powder mass, alkali content was 11%, water glass modulus was 1.4, and water-solid ratio was 0.35. Excessive OPC in geopolymers may lead to the formation of relatively lower terpolymeric binders than hydrated calcium-based binders. The chemical compositions of the GFRP powder, FA, SS, and OPC were determined by X-ray fluorescence (XRF) spectroscopy, and the results are given in Table 1. The particle sizes of the raw materials were measured using a laser particle size analyzer, and the results are listed in Table 2.

The alkaline solution was a combination of sodium silicate (Na₂SiO₃) with a modulus ratio (M_s) of 3.2 (where M_s = SiO₂/Na₂O, Na₂O = 8.54%, SiO₂ = 27.3%) and sodium hydroxide (NaOH) prepared by dissolving NaOH solids (96% purity) in water. In this work, the 19.5 M NaOH solution consisted of 778 g of NaOH solids per liter of water. The alkaline solution was prepared approximately 24 h prior to use.

Natural river sands with a fineness modulus of 2.7 were used as fine aggregates, and crushed limestone aggregates with diameter of 15–30 mm were used as coarse aggregates. The specific densities of the fine and coarse aggregates were 2.65 and 2.67 g/cm³, respectively.

Table 4 Taguchi OA₉ (3⁴) orthogonal array.

Trial	Factor A	Factor B	Factor C	Factor D
G1	1	1	1	1
G2	1	2	2	2
G3	1	3	3	3
G4	2	1	2	3
G5	2	2	3	1
G6	2	3	1	2
G7	3	1	3	2
G8	3	2	1	3
G9	3	3	2	1

2.2. Mixture design of geopolymer paste

The mixture proportion of the geopolymer paste was determined based on the orthogonal experimental design method. Four factors related to strength are listed in Table 3, including activator concentration, L/S, activator solution modulus, and GFRP powder content. The activator concentration is the mass fraction of the initial Na₂SiO₃ solution and the added NaOH solids to the modified Na₂SiO₃ solution. The use of a higher activator concentration enhances the incorporation of Si and Al into the gel structure, thus increasing the geopolymerization and the stiffness of geopolymers [39]. However, excess hydroxide ion concentration may cause aluminosilicate product precipitation at early stage, resulting in a decrease in strength of geopolymer [39]. The modulus of alkali activator is the molar ratio of SiO₂ to Na₂O in alkaline solution. Zhou et al. [40] have stated that cracks are generated in the microstructure of geopolymer when the modulus of alkali activator exceeds 1.8, and the optimal conditions for fly ash based-geopolymer paste (the content of Al₂O₃ below 25%) is given as curing temperature of 80 $^{\circ}\text{C},$ Si to Al ratio of 2:1 and activator solution modulus of 1.5. High amount of liquid content than the solids in the geopolymer mixture leads to the decrease in the compressive strength because of the reduced contact between the activating solution and the

Table 5 Geopolymer mixture.

Mix	Fly ash (kg/ m ³)	GFRP powder (kg/m³)	Steel slag (10%) (kg/m³)	OPC (10%) (kg/m ³)	NaOH (kg/ m³)	Na ₂ SiO ₃ (kg/m ³)	Water (kg/m³)	PS (kg/ m ³)	Mass ratio of SiO_2 to Al_2O_3	Content of SiO_2 and Al_2O_3
G1	883.2	294.4	147.2	147.2	104.1	565.8	286.9	29.44	2.13	63.49
G2	736.0	441.6	147.2	147.2	107.7	665.1	331.2	29.44	2.23	59.88
G3	588.8	588.8	147.2	147.2	108.9	767.1	375.1	29.44	2.36	56.26
G4	588.8	588.8	147.2	147.2	106.7	658.7	191.4	29.44	2.36	56.26
G5	883.2	294.2	147.2	147.2	109.8	773.4	220.8	29.44	2.13	63.49
G6	736.0	441.6	147.2	147.2	155.6	845.4	250.2	29.44	2.23	59.88
G7	736.0	441.6	147.2	147.2	101.1	712.2	143.5	29.44	2.23	59.88
G8	588.8	588.8	147.2	147.2	145.8	792.5	165.6	29.44	2.36	56.26
G9	883.2	294.4	147.2	147.2	148.3	915.3	187.6	29.44	2.13	63.49
G10	736.0	441.6	147.2	147.2	113.38	699.9	143.5	29.44	2.23	59.88

Note: PS means polycarboxylate superplasticizer.

Table 6Test results of trial mixes of geopolymer paste.

Mix	Initial setting time (min)	Final setting time (min)	Flowability (mm)	Compressive strength (MPa)			Flexural strength (MPa)		
				3d	7d	28d	3d	7d	28d
G1	172	205	183	3.76	5.98	8.54	1.76	2.06	2.32
G2	185	255	221	3.51	6.30	9.23	1.46	1.91	2.17
G3	195	270	205	3.13	6.42	9.85	1.95	2.06	2.13
G4	120	155	135	5.54	8.47	16.34	2.37	2.47	3.03
G5	165	205	187	3.88	5.92	9.14	1.95	1.98	2.06
G6	205	305	235	4.80	6.01	10.95	1.65	2.43	2.81
G7	140	170	143	6.54	9.10	18.15	1.68	2.51	3.29
G8	125	165	141	2.49	6.50	10.21	1.17	1.91	2.85
G9	195	285	224	3.22	6.67	12.43	1.35	1.98	2.70
G10	150	145	190	6.33	9.42	19.34	1.72	2.47	3.26

Table 7 Geopolymer concrete mixture (kg/m³).

Mix	FA (kg/ m ³)	GFRP powder (kg/m³)	OPC (kg/m ³)	SS (kg/ m ³)	NaOH solids (kg/m³)	Na ₂ SiO ₃ solution (kg/ m ³)	Water (kg/m³)	Fine aggregate (kg/m³)	Coarse aggregate (kg/m³)	PS (kg/ m ³)	s/a	a/ b
GC-	298.38	-	37.30	37.30	28.64	174.25	35.81	680.29	1109.94	7.46	0.38	4.8
GC- 1	186.49	111.89	37.30	37.30	28.64	174.25	35.81	680.29	1109.94	7.46	0.38	4.8
GC- 2	186.49	111.89	37.30	37.30	28.64	174.25	35.81	590.78	1199.45	7.46	0.33	4.8
GC- 3	186.49	111.89	37.30	37.30	28.64	174.25	35.81	769.80	1020.43	7.46	0.43	4.8
GC- 4	202.13	121.28	40.43	40.43	31.05	188.87	38.81	660.55	1077.74	8.09	0.38	4.3
GC- 5	173.09	103.85	34.62	34.62	26.59	161.73	33.23	697.19	1137.53	6.92	0.38	5.3

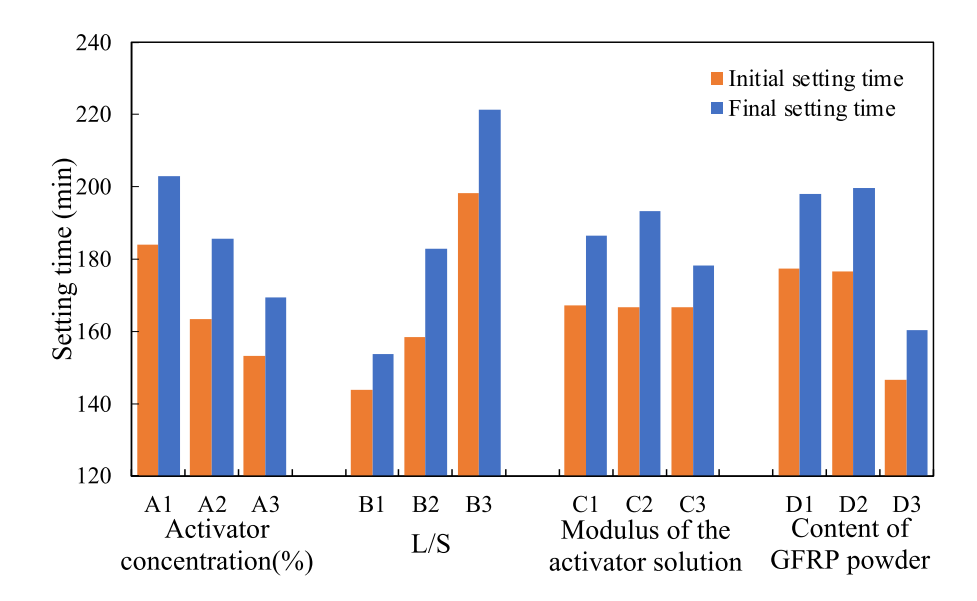


Fig. 2. Relationship between setting time and four mix factors for GFRP powder/FA-based geopolymer pastes.

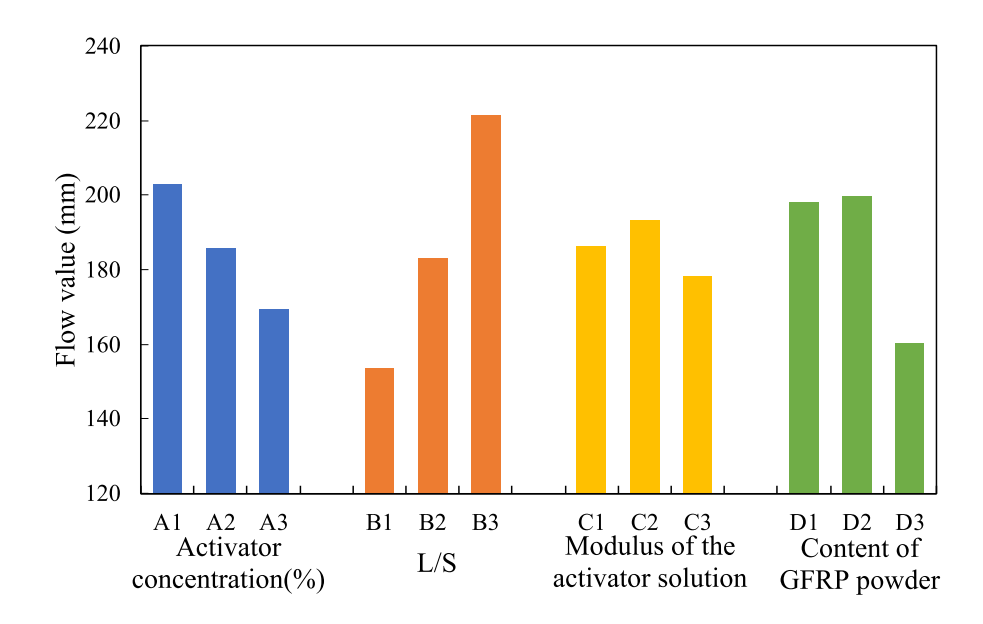


Fig. 3. Relationship between flow value and four mix factors for GFRP powder/FA-based geopolymer pastes.

reacting material [41]. Therefore, the activator concentration is varied as 70%, 80% and 85%, respectively, the L/S is varied as 0.65, 0.75 and 0.85, respectively, and modulus of the activator solution is varied as 1.2, 1.3 and 1.4, respectively. The additive of a small amount of epoxy resin (around 10 wt%) can improve the mechanical performance of geopolymers [19,20]. The GFRP powder content is varied as 20%, 30% and 40%, respectively.

The Taguchi orthogonal array for the full factorial experiment is shown in Table 4. For all mixtures, the weight amounts of SS, OPC, and polycarboxylate superplasticizer (PS) in the binder are 10%, 10%, and 2%, respectively. The proportions of each mixture are listed in Table 5.

The Na_2SiO_3 solution adjusted by NaOH was used as the alkali activator solution. According to the composition content of the initial Na_2SiO_3 solution ($Na_2O=8.54\%$, $SiO_2=27.3\%$) and the NaOH solids (96% purity) used in this study, formula (1) can be obtained to calculate

the mass of NaOH solids added in the initial Na_2SiO_3 solution to obtain the alkaline solution with target modulus. To obtain the L/S required for the test, formula (2) is used to calculate the additional water in geopolymer paste.

$$m_{NAOH} = \frac{1.34\omega_{Na_2O} \times \left(\frac{M}{C} - 1\right)}{1 + 1.34\omega_{Na_2O}\left(\frac{M}{C} - 1\right)} m_{soildpowder} \times A \times B$$
(1)

$$m_{\rm H_2O} = m_{soildpowder} \times B \times (1 - A)$$
 (2)

where $m_{\rm NaOH}$ is the mass of NaOH solids (g), $m_{\rm H2O}$ is the mass of additional deionized water (g), $m_{\rm solidpowder}$ is the total mass of solid powder, which is equal to the mass of GFRP powder, FA, SS and OPC (g), M is the modulus of the initial Na₂SiO₃ solution, A is the activator concentration,

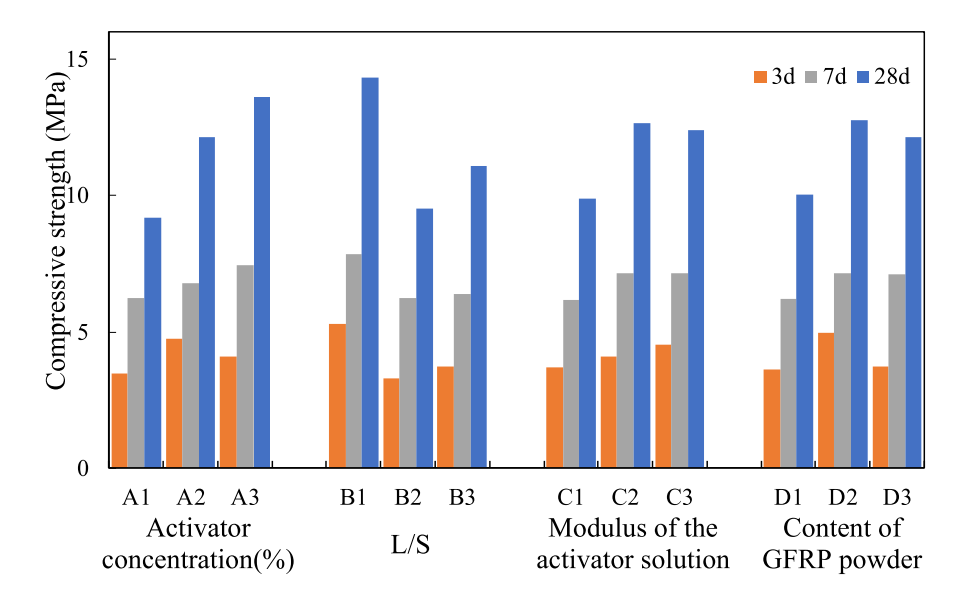


Fig. 4. Relationship between compressive strength and four mix factors for GFRP powder/FA-based geopolymer pastes.

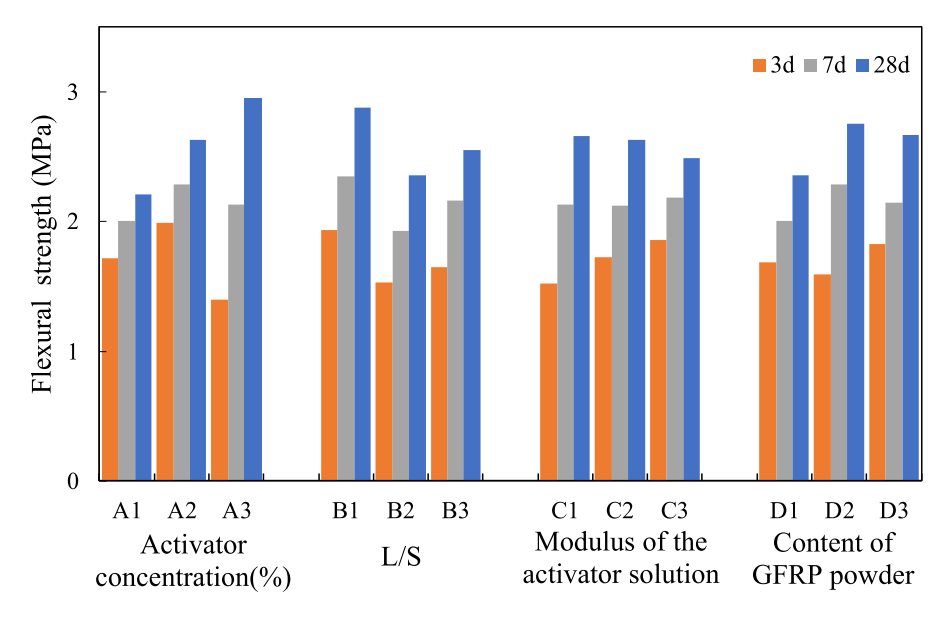


Fig. 5. Relationship between flexural strength and four mix factors for GFRP powder/FA-based geopolymer pastes.

B is L/S, C is the target modulus of alkaline solution, $\omega_{\rm Na2O}$ is the mass fraction of Na₂O in the initial Na₂SiO₃ solution.

2.3. Preparation of geopolymer concrete

The geopolymer paste test results (Table 6) indicate that the optimal combination of geopolymer mixture with the highest 28-day compressive strength is given as an activator concentration of 85%, L/S of 0.65, activator solution modulus of 1.3, and GFRP powder content of 30 wt%. This optimal mixture was then used to prepare geopolymer concrete. The effects of sand-to-aggregate ratio (s/a = 0.33, 0.38, 0.43) and aggregate to binder ratio (a/b = 4.3, 4.8 and 5.3) were taken into account in the geopolymer concrete mixture design, as shown in Table 7. A geopolymer concrete specimen without GFRP powder (GC-0) was also prepared as a reference point for comparison purposes (see Table 7).

According to the mixture of geopolymer concrete with 2% PS, the mass of binder solids in the geopolymer concrete can be determined as

$$m_{solidpowder} = \frac{m_{geopolymerconcrete}}{(1.02 + a/b + B)}$$
(3)

Substituting formula (3) into formula (2), the additional water in geopolymer concrete can be obtained.

Where *m*_{geopolymerconcrete} is the mass of geopolymer concrete (kg), a/b is aggregate-to-binder ratio in geopolymer concrete.

After casting, the geopolymer concrete specimens and molds were covered with plastic film to prevent moisture loss and then cured at room temperature for 24 h. After removal from their molds, the specimens were cured in a standard curing room at 20 \pm 2 $^{\circ}\text{C}$ at a relative humidity (RH) of 95% until the corresponding age.

Based on the compressive test results, the geopolymer concrete

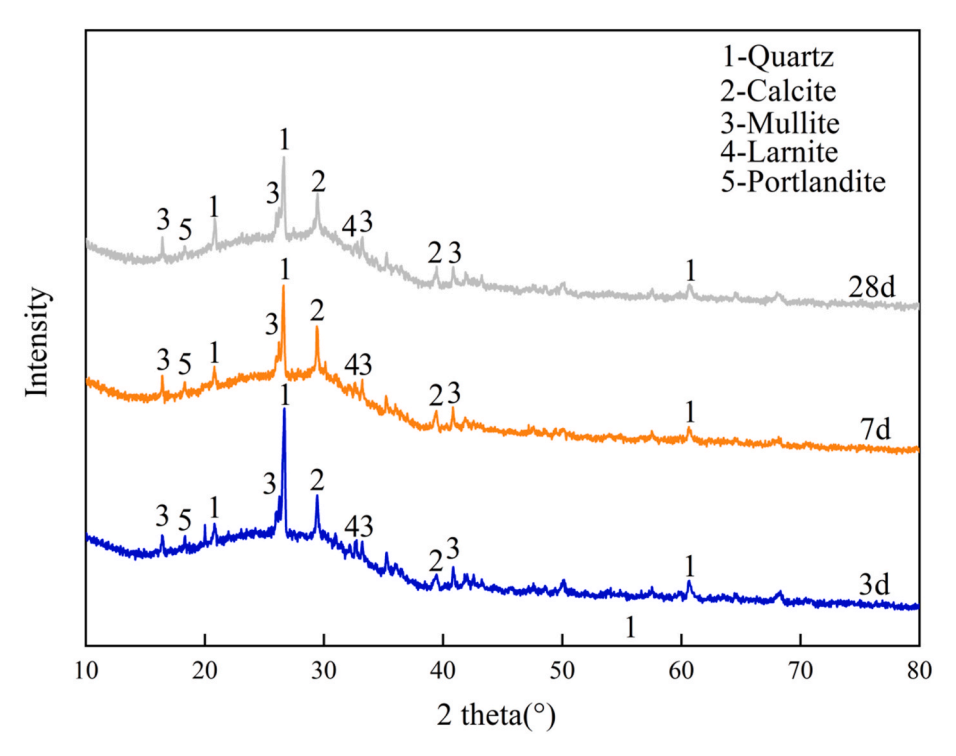


Fig. 6. XRD analysis of optimal GFRP powder/FA-based geopolymer mixtures (G10).

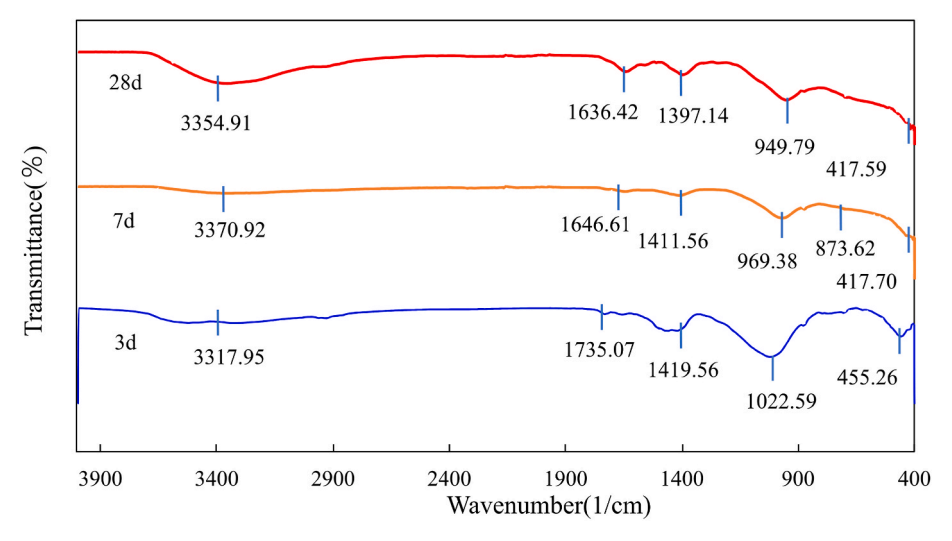


Fig. 7. FTIR spectra of optimal GFRP powder/FA-based geopolymer mixtures (G10).

mixture with the highest compressive strength at ambient temperature was applied to investigate the effects of high temperature. The high-temperature behavior of the specimens without GFRP powder was also tested as a reference.

2.4. Experimental program

2.4.1. Workability

The initial and final setting times of the geopolymer paste were determined in accordance with Chinese standard GB/T 1346–2011 [42]. Flowability tests of the fresh geopolymer paste were conducted in accordance with Chinese standard GB/T 8077–2012 [43]. The initial and final setting times and flowability of the geopolymer concrete were determined in accordance with Chinese standard GB/T 50080–2016 [44]. The reported setting time and flowability values represent the average of three measurements at room temperature.

2.4.2. Mechanical tests of geopolymer paste

The compressive and flexural strengths were examined at ages of 3, 7, and 28 days to evaluate the mechanical characteristics of the hardened geopolymer pastes using a universal testing machine with a capacity of 2000 kN. The flexural strength was determined following the three-point bend method on prismatic specimens with dimensions of 40 \times 40 \times 160 mm. The clear span between two supporting points was maintained at 100 mm. Three specimens of each formulation were tested in accordance with Chinese standard GB/T 17671–1999 [45]. Compressive strength tests were conducted on the two broken parts of the prismatic specimens obtained from the flexural strength test. The loading rate was 2.4 kN/s under a loading area of 40 \times 40 mm.

2.4.3. Mechanical tests of geopolymer concrete at ambient and high temperatures

All of the geopolymer concrete specimens in the molds were cured at

Table 8Test results of geopolymer concrete at ambient temperatures.

Mix	Initial setting time (min)	Final setting time	ing (mm)		pressive gth (MPa	Flexural strength (MPa)	
		(min)		3d	7d	28d	28d
GC- 0	293	351	197	6.5	8.5	31.8	3.71
GC- 1	275	330	205	7.6	10.9	36.5	4.74
GC- 2	285	337	210	7.2	10.3	35.4	4.79
GC- 3	270	325	198	7.7	11.2	35.8	4.77
GC-	288	343	207	7.1	10.4	34.2	4.34
GC- 5	273	336	195	8.5	11.1	32.7	4.92

room temperature for 24 h. The specimens were then removed from the molds and cured at $20\pm2\,^{\circ}\text{C}$ and 95% RH in a steam curing room for 28 days. A muffle furnace designed for a maximum temperature of 1050 $^{\circ}\text{C}$ was used for heating the specimens at 300, 600, and 900 $^{\circ}\text{C}$. The specimens were heated to the target temperature at a heating rate of 5 $^{\circ}\text{C}/\text{min}$, and the target temperature was held constant for 3 h to achieve a thermal steady state. After reaching the target temperature, the specimens were cooled at room temperature for 24 h before weighing. These compressive strength and flexural strength tests were performed in accordance with Chinese standard GB/T50081-2019 [46]. The mechanical properties of the reference specimens at the room temperature were also measured for comparison.

2.4.4. Microstructure analysis

The mineral phases of the geopolymer were identified using XRD. The wave numbers of geopolymer from 400 to $4000~\rm cm^{-1}$ were recorded using FTIR. Microstructure changes of geopolymer concrete specimens at different ages and temperatures were examined by SEM coupled with FDS

3. Results and discussion

3.1. Properties of geopolymer materials at ambient temperature

3.1.1. Geopolymer paste

3.1.1.1. Setting times. The test results of the geopolymer pastes are listed in Table 6. The initial setting time of fresh paste containing GFRP powder was in the range of 120–205 min, and the final setting time was in the range of 165–305 min. This is consistent with the requirements for ordinary Portland cement in standard GB 175–2007, which state that the initial setting time should be longer than 45 min and the final setting time should be shorter than 600 min.

The relationship between setting time and the four mixture factors is shown in Fig. 2. The response index for each factor represents the average of the three values for the trial mixtures containing the particular factor. The influence of factor B (L/S) on the setting time is notably greater than those of the other factors. Both the initial and final setting time increased with increasing L/S, and decreased with increasing activator concentration. The higher water content associated with the increased alkaline solution content may retard the geopolymerization process, whereas the increased activator concentration can improve the dissolution rate of the aluminosilicate precursors, thus enhancing the geopolymerization process. Increasing the GFRP powder content from 20 to 30 wt% had an insignificant effect on the initial and final setting times, but a further increase to 40 wt% reduced the setting time. The low-calcium FA-based geopolymer paste took more than 24 h before showing any sign of setting due to the slow chemical reaction rate at room temperature (20–23 °C) [47]. The setting time primarily depends on the formation of C-S-H or C-A-S-H gel products [48]. High CaO contents may accelerate the geopolymer hydration reaction [49]. Replacing low-calcium FA with GFRP powder could accelerate the geopolymerization process, thus decreasing the setting time. The activator solution modulus in the range of 1.2-1.4 had an insignificant effect on the initial and final setting times, indicating that the effect of this factor on the setting time does not need be considered when using an activator solution modulus in a reasonable range.

3.1.1.2. Flowability. The relationship between the flow value and four

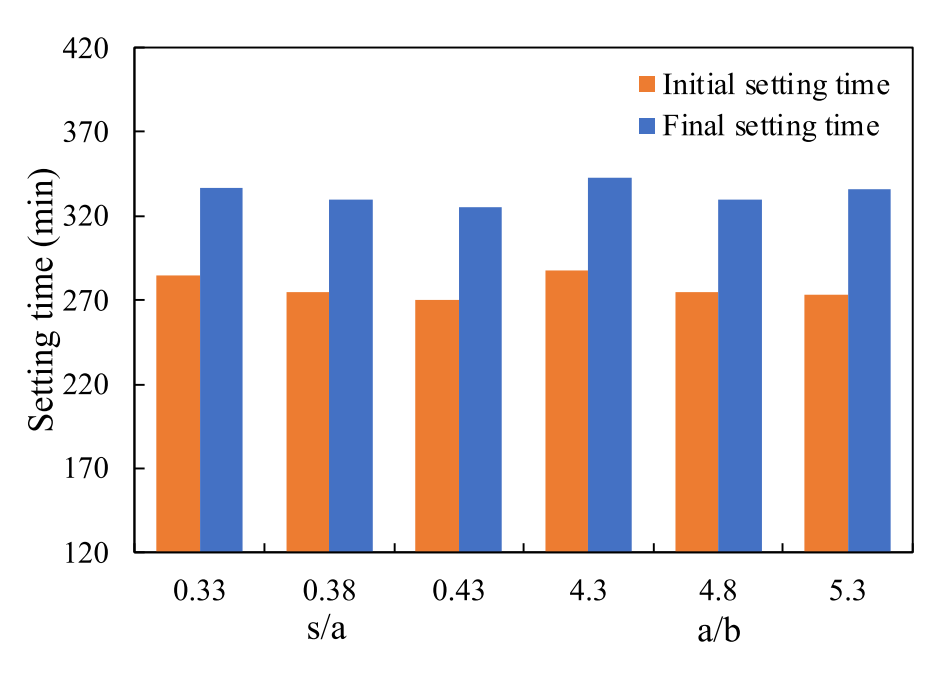


Fig. 8. Influences of s/a and a/b on the setting time of GFRP powder/FA-based geopolymer concrete.

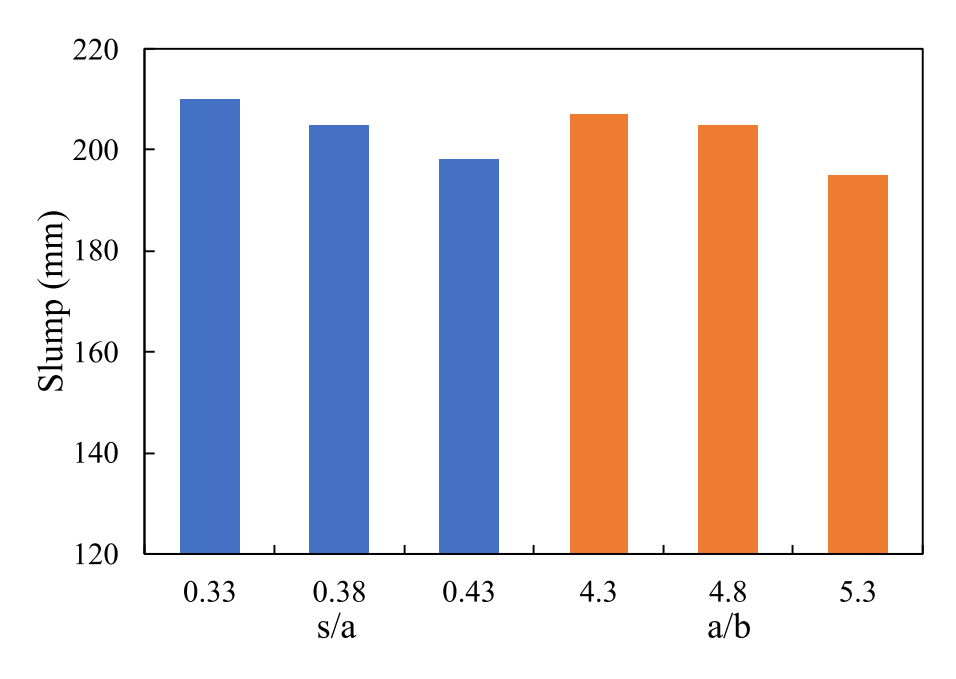


Fig. 9. Influences of s/a and a/b on the slump of GFRP powder/FA-based geopolymer concrete.

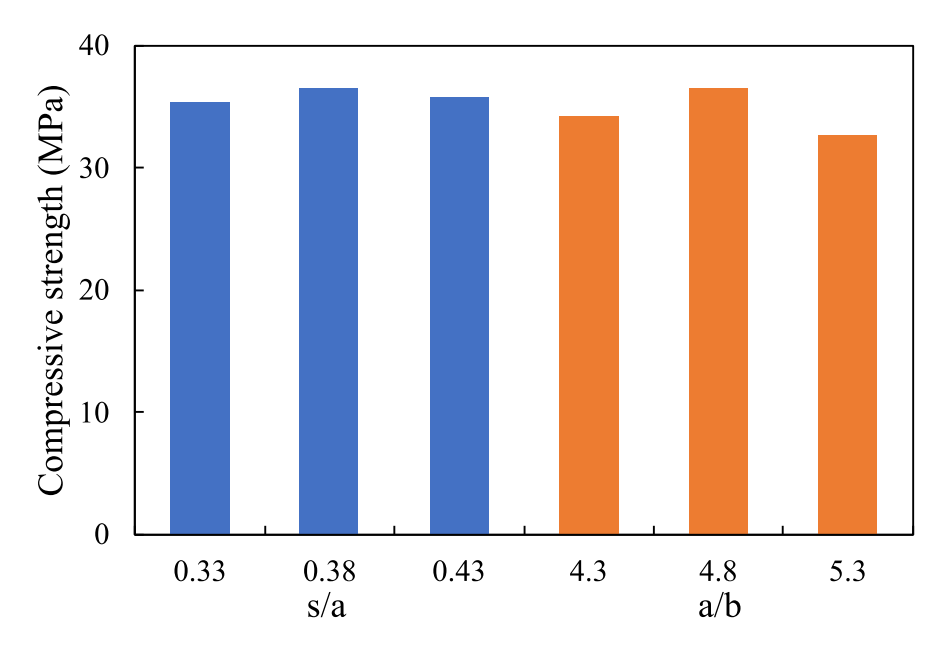


Fig. 10. Influences of s/a and a/b on the compressive strength of GFRP powder/FA-based geopolymer concrete.

mixture factors is shown in Fig. 3. The flow value of the GFRP powder/FA-based geopolymer pastes was in the range of 135–235 mm. The effect of factor B (L/S) on the flowability was more significant than the other factors. The flow value increased with increasing L/S, and decreased with increasing activator concentration. This is because higher L/S or lower activator concentration can retard the chemical reaction rate of aluminosilicate materials with activator solution, thus enhancing the flowability. Increasing the GFRP powder content from 20 to 30 wt% had an insignificant effect on the flow value, but further increasing the content led to a reduced flow value. This is mainly because the CaO content in GFRP powder/FA-based geopolymers increases with increasing GFRP powder content, thus accelerating the chemical reaction rate of the aluminosilicate raw materials with the activator solution.

The activator solution modulus in the range of 1.2–1.4 had an insignificant influence on the flowability. Hence, the role of the activator solution modulus does not need to be considered as a flowability indicator when the modulus is within a reasonable range.

3.1.1.3. Compressive strength. The relationship between the compressive strength of the geopolymer pastes and four mixture factors is shown in Fig. 4. The four mixture factors have an insignificant effect on the early compressive strength, whereas the effect of factor B (L/S) on the 28-day compressive strength was more significant than the other factors. Both the early and 28-day compressive strengths of the geopolymers with an L/S ratio of 0.65 were higher than those of the geopolymers with L/S ratios of 0.75 and 0.85. This is because higher solution content

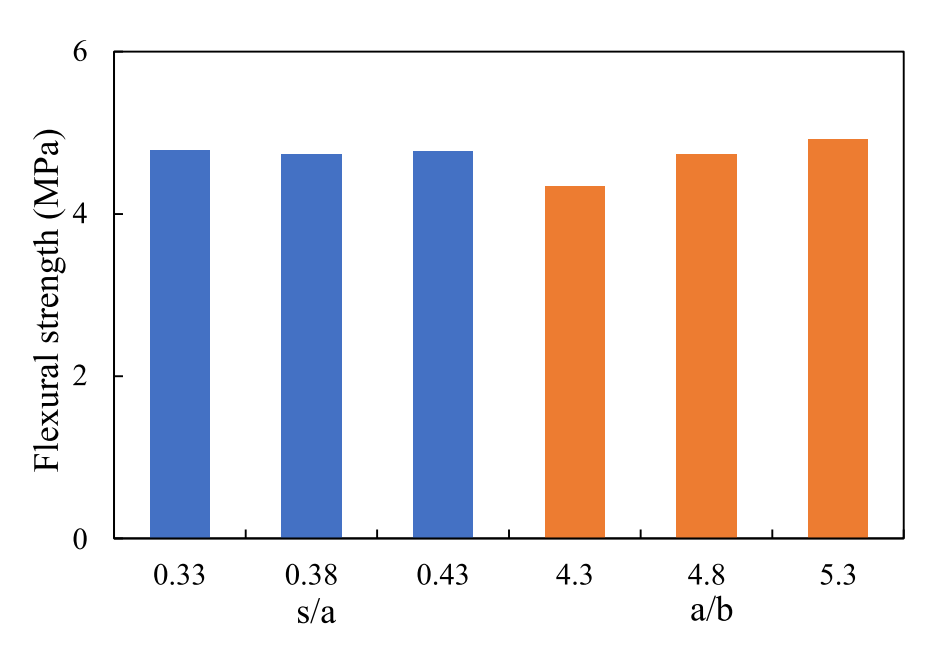


Fig. 11. Influences of s/a and a/b on the flexural strength of GFRP powder/FA-based geopolymer concrete.

increases the water content, which negatively affects the compressive strength [50]. Increasing the alkali concentration enhanced the 28-day compressive strength of the geopolymers. Higher alkali concentration may thus accelerate the dissolution rates of GFRP powder and FA, thus improving the development of the geopolymerization process. The activator solution modulus had an insignificant effect on the compressive strength when in the range of 1.2–1.4.

Geopolymer pastes with 30 wt% GFRP powder were found to have a higher compressive strength than those with 20 or 40 wt% GFRP powder. This may be attributed to the resin impregnated on the surface of glass fiber powder, which hinders the further dissolution of Si and Al. In general, the 3-day compressive strength of the geopolymers was approximately one-third of their 28-day compressive strength, and the 7-day compressive strength of geopolymers was more than half of their 28-day compressive strength. As mentioned in Ref. [51], Al₂O₃ exhibits a higher dissolution rate in the early age and can enhance the chemical reaction rate of the C-A-S-H gel products. The low Al₂O₃ content in the precursors therefore caused the low early compressive strength of the geopolymers. The geopolymer having low-calcium FA only as the binder was very weak to produce a reasonable strength even after three days of casting when cured at ambient temperature (20-23 °C) [47]. The reactivity of the GFRP powder and SS were gradually stimulated with increasing curing time, thus improving the compressive strength of the geopolymers.

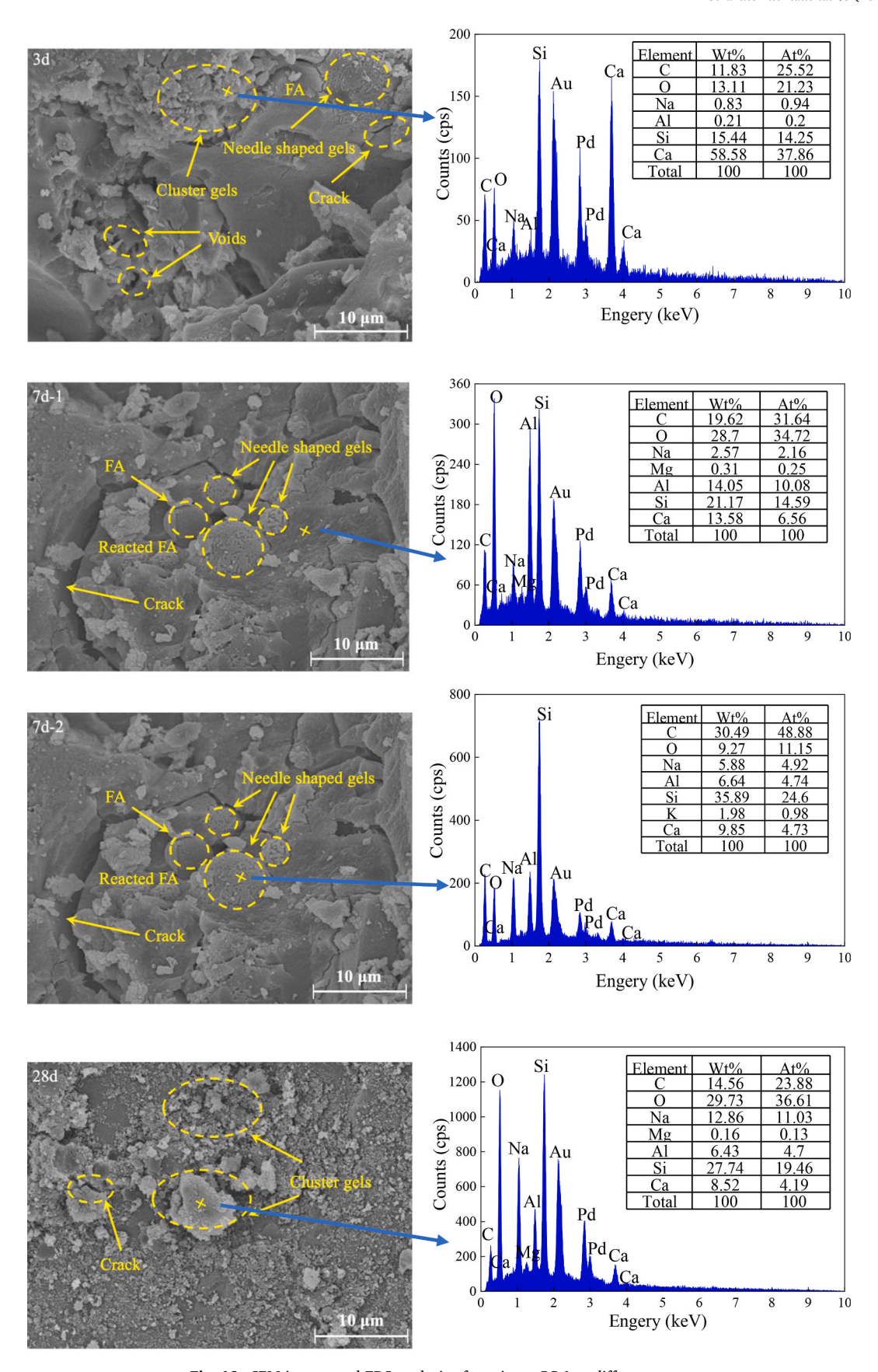
3.1.1.4. Flexural strength. Fig. 5 shows that the variation of flexural strength with reference to the four mixture factors is similar to that of compressive strength. The highest ratios of compressive strength to flexural strength (RCF) of the geopolymers at 3, 7, and 28 days were 3.89, 3.63, and 5.52, respectively. The RCF tends to increase with increasing curing time. The RCF is an important indicator that can reflect geopolymer brittleness. Larger RCF values imply that the material is more brittle. The highest RCF values of the FA/SS-based geopolymers were 6.77, 6.92, and 7.46, respectively [52], which are considerably higher than those of the GFRP powder/FA based geopolymers. This indicates that the resin in the GFRP powder can improve the geopolymer brittleness. Moreover, the early flexural strength of the geopolymers developed more rapidly than the early compressive strength.

Based on the 28-day strength test results, the optimal combination of

GFRP powder/FA-based geopolymer pastes was A3B1C2D2, including an activator concentration of 85%, L/S of 0.65, activator solution modulus of 1.3, and GFRP powder content of 30 wt%. The workability and mechanical properties of the optimal GFRP powder/FA-based geopolymer paste were consequently obtained, as listed in Table 6. Under these conditions, the final 28-day compressive and flexural strengths of the geopolymer paste were 19.34 and 3.26 MPa, respectively.

3.1.1.5. Microstructures. The XRD results of the optimal GFRP powder/FA-based geopolymer pastes at 3, 7, and 28 days are presented in Fig. 6. The crystalline phases of the hardened pastes at the different curing ages are mainly quartz (SiO₂), calcite (CaCO₃), mullite (Al₆Si₂O₁₃), larnite, and portlandite (Ca(OH)₂). The co-existing quartz and mullite are due to the effect of the FA components, which indicates that not all of the quartz and calcite participate in the geopolymerization. The quartz peak intensity decreased with increasing curing age, which indicates that Si ions had dissolved in the alkaline solution during geopolymerization. The presence of portlandite is due to GFRP powder inclusions. Owing to the presence of CaO in the raw materials, the broad amorphous humps between 20° and 35° are expected to depict the presence of C–S–H, C-A-S-H, and N-A-S-H gels in the binder [33]. No new crystalline phases formed with increasing curing time because the hydration and polymeric products are mainly amorphous phases.

The FTIR spectra of the optimal GFRP powder/FA-based geopolymer mixtures at ages of 3, 7, and 28 days are shown in Fig. 7. The bands observed at 3317–3371 and 1636–1735 cm⁻¹ are assigned to the antisymmetric/symmetric stretching vibration of O–H. The absorption band at 1397–1420 cm⁻¹ is related to the vibration of O–C–O bonds caused by carbonization. The bands observed around 1000 cm⁻¹ can be assigned to the anti-stretching vibrations of Si–O-T (T = Si or Al), which are attributed to the development of an amorphous N-A-S-H gel and C–S–H gel network [53]. These bands shift toward higher wavenumbers with increasing curing time, which indicates that the formed gels had acquired higher degrees of crosslinking. Higher geopolymerization degrees led to higher geopolymer strength. The bands at 455 cm⁻¹ are assigned to the flexural vibrations of the Si–O–Si bonds, reflecting the gel phase structure in the FA-based geopolymers [54].



 $\textbf{Fig. 12.} \ \ \textbf{SEM} \ \ \textbf{images} \ \ \textbf{and} \ \ \textbf{EDS} \ \ \textbf{analysis} \ \ \textbf{of} \ \ \textbf{specimen} \ \ \textbf{GC-1} \ \ \textbf{at} \ \ \textbf{different} \ \ \textbf{ages}.$

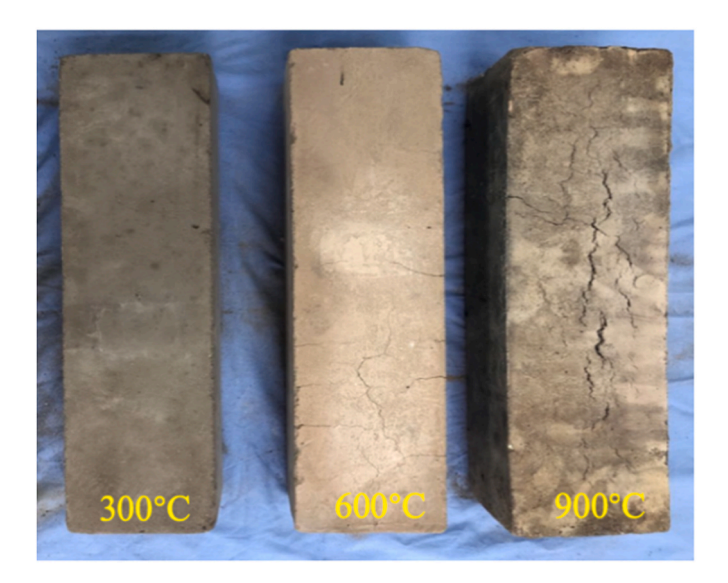


Fig. 13. Specimens GC-1 after exposure to elevated temperatures.

Table 9Test results of geopolymer concrete after exposure to high temperatures.

Specimens		Compressive strength (MPa)	Flexural strength (MPa)	Mass loss ratio (%)	
GC-	25 °C	31.8	3.7	_	
0	300 °C	21.1	2.1	5.8	
	600 °C	13.3	1.8	6.1	
	900 °C	8.7	0.9	23.5	
GC-	25 °C	36.5	4.7	-	
1	300 °C	24.5	3.2	6.4	
	600 °C	16.1	2.4	6.7	
	900 °C	9.1	1.0	21.0	

3.1.2. Geopolymer concrete

3.1.2.1. Workability. The geopolymer concrete test results are listed in Table 8. For the same s/a and a/b values, the specimens with GFRP powder (GC-1) exhibited slightly shorter setting times than the GFRP powder-free specimens (GC-0) because the higher CaO content in specimen GC-1 accelerated the geopolymer hydration reaction. As shown in Fig. 8, s/a and a/b values in the range of 0.33–0.43 and 4.3–5.3, respectively, had an insignificant influence on the setting time. Hence, the roles of s/a and a/b do not need to be considered as a setting time indicator when these ratio values are within a reasonable range.

The higher low-calcium FA content resulted in a higher slump of the geopolymer concrete [50]. However, the slump of GC-1 was slightly higher than that of GC-0 due to the low-absorbent nature of the GFRP powder. As shown in Fig. 9, the slump of the GFRP powder/FA-based geopolymer concrete slightly decreased with increasing s/a. Excessive amounts of sand reduced the mixture workability because the entire surface of the sand and coarse aggregates was too large to be covered by the geopolymer binder [55]. The slump of the GFRP powder/FA-based geopolymer concrete also decreased with increasing a/b. This can be attributed to the reduced viscosity of the geopolymer concrete with decreased binder content.

3.1.2.2. Compressive strength. For identical s/a and a/b ratios, the early and 28-day compressive strength of the geopolymer concrete containing 30% GFRP powder as a replacement for FA (GC-1) were 15%–28% higher than those of the geopolymer concrete without GFRP powder (GC-0). The geopolymer concrete having low-calcium FA only as the binder reacted slowly to develop strength when cured at 20–23 °C [41]. The 28-day compressive of geopolymer concrete containing 30% GFRP

powder was 35% higher than that of geopolymer concrete having low-calcium FA only, as reported in Ref. [41]. Incorporating no more than 30% of glass powder in the geopolymer matrix was found to strengthen the bonding between the aggregates and binder in the transition zone [56]. Further increasing the GFRP powder content resulted in a high silica/alumina ratio, thus leading to the formation of an inferior aluminosilicate product and reduction of the compressive and flexural strengths [16].

Figs. 10 and 11 show that both s/a and a/b had an insignificant influence on the compressive strength when within a reasonable range. The specimen with s/a = 0.38 and a/b = 4.8 (GC-1) yielded the highest compressive strength among all of the tested specimens.

3.1.2.3. Flexural strength. For identical s/a and a/b ratios, the 28-day flexural strength of the geopolymer concrete containing 30% GFRP powder as a replacement for FA (GC-1) was 28% higher than that the geopolymer concrete without GFRP powder (GC-0). The increased flexural strength upon incorporating an appropriate amount of GFRP powder is due to the pozzolanic nature, improvement in the interfacial transition zone nature, and filling ability of the GFRP waste powder [16]. Excessive GFRP waste powder had adverse effects on the geopolymer mixture's flexural strength due to the brittle characteristics of the glass fiber powder. s/a and a/b values in the range of 0.33–0.43 and 4.3–5.3, respectively, had an insignificant influence on the flexural strength of the GFRP powder/FA-based geopolymer concrete. The specimen with s/a = 0.38 and a/b = 5.3 (GC-5) yielded the highest flexural strength among all of the tested specimens.

3.1.2.4. Microstructures. SEM images of specimen GC-1 at ages of 3, 7, and 28 days after compression are presented in Fig. 12. The microstructure of specimen GC-1 at 3 days comprised cluster gels, needle-shaped gels, unreacted FA particles, voids, and cracks. The EDS results of the cluster network gel products of this specimen indicate that Ca, Si, O, and C were the principal elements in the gel products with minor amounts of Na and Al. Because the precursors contain a considerable amount of SiO₂ and CaO, Si and Ca ions were released during the geopolymerization to form C–S–H gel products. The Al/Si, Na/Si, and Ca/Si atomic ratios for the gel products of this specimen were 0.014, 0.066, and 2.66, respectively, indicating that most of the gel products contained C–S–H gel. C ions were released from the unsaturated polyester resin in the GFRP powder because the resin matrix contains –COOH, –CH₃, and –CH.

The microstructure of specimen GC-1 at 7 days exhibited more needle-shaped gels surrounded and bound by FA particles than the 3-day specimen due to the development of the geopolymer matrix [52]. The EDS results of specimen GC-1 at 7 days indicate Al/Si, Na/Si, and Ca/Si atomic ratios for the geopolymer matrix of 0.69, 0.15, and 0.45, respectively. The Al/Si, Na/Si, and Ca/Si atomic ratios for the needle-shaped gels in this specimen were 0.19, 0.2, and 0.19, respectively. The considerable amounts of Si, Al, and Na were related to the polymerization reactions that produced strong Si–Al and Na–Al–Si bonds [57], which indicates that the N-A-S-H gel products formed coexisting with C–S–H or C-A-S-H gels during geopolymerization. The Ca/Si atomic ratio of specimen GC-1 at 7 days was substantially lower than that at 3 days, which can be related to the increased dissolution of Ca ions.

In terms of the microstructure of specimen GC-1 at 28 days, the unreacted FA was undiscernible and a large amount of cluster gels was found in the matrix, indicating a high degree of geopolymerization. The EDS results of the cluster gels of specimen GC-1 at 28 days, showed Al/Si, Na/Si, and Ca/Si atomic ratios of 0.24, 0.57, and 0.22, respectively. An Al/Si ratio in the range of 0.2–0.4 is therefore considered to be suitable for mechanical strength development [27].

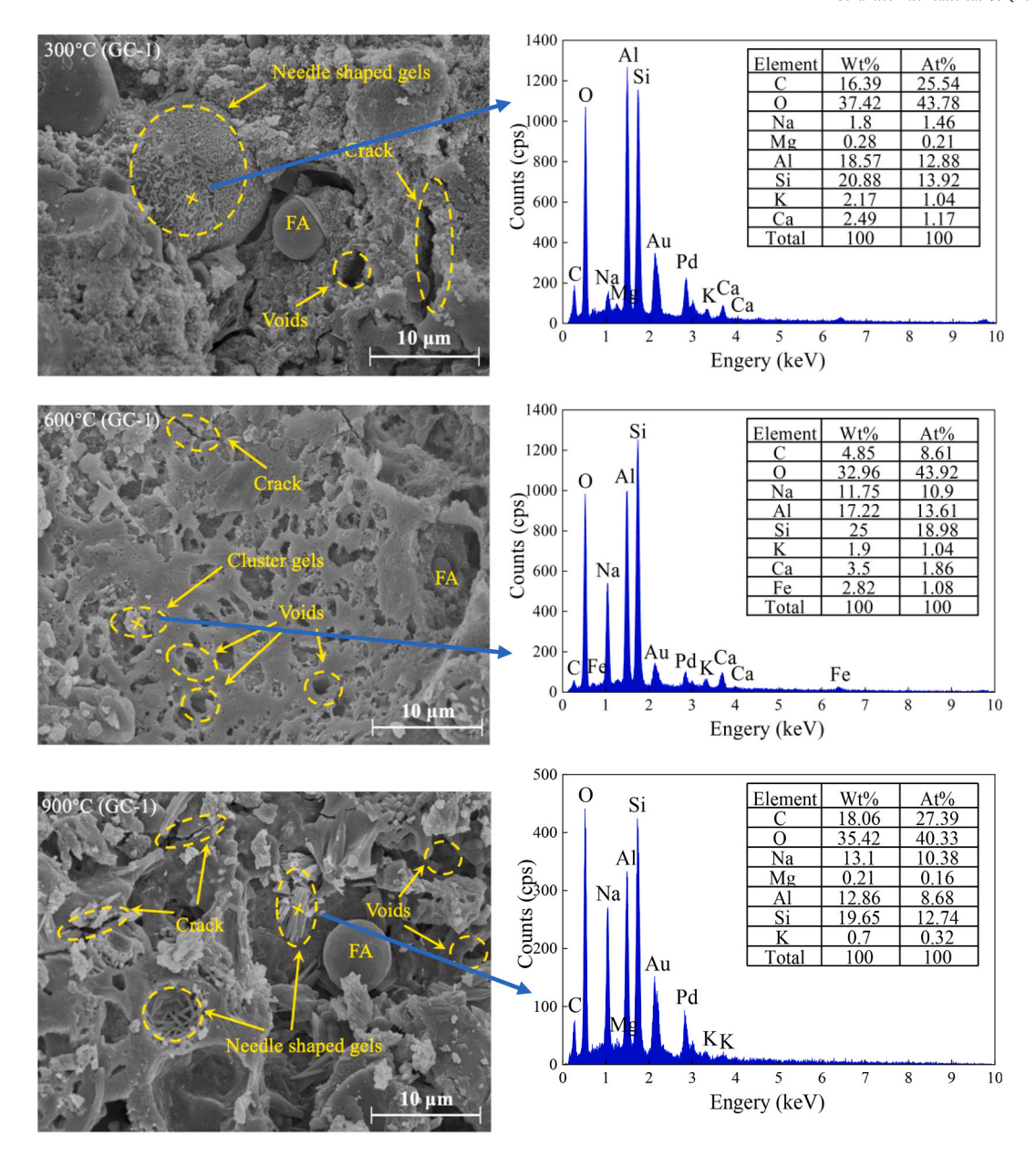


Fig. 14. SEM images and EDS analysis of specimen GC-1 after exposure to elevated temperatures.

3.2. Properties of geopolymer concrete after high-temperature exposure

3.2.1. Mechanical properties

Specimen GC-1 exhibited the highest compressive strength at ambient temperature among the tested geopolymer concrete specimens, and was thus used to investigate the effect of high temperature. The high-temperature behavior of a specimen without GFRP powder (GC-0) was tested as a reference. The surfaces of specimen GC-1 after high-temperature exposure are shown in Fig. 13. The color of the samples exposed to 300 $^{\circ}\text{C}$ remained nearly unchanged and no cracks were noted on their surfaces. In contrast, the samples exposed to 600 $^{\circ}\text{C}$ underwent a significant color change and several cracks were clearly observed on the surface. When the temperature was increased to 900 $^{\circ}\text{C}$, the cracks widened and connected with each other.

The properties of specimens GC-0 and GC-1 after high-temperature exposure are listed in Table 9. The compressive strength of specimen GC-1 exposed to 300, 600, and 900 $^{\circ}$ C decreased by 33%, 56%, and 75%, respectively, compared with the ambient temperature value, which is similar to the results of specimen GC-0. The flexural strength losses for

specimen GC-1 were 32% and 49% at 300 and 600 °C, respectively, which were lower than those of specimen GC-0. The flexural strength loss for specimen GC-1 at 900 °C was 79%, which was slightly higher than that of specimen GC-0 at 900 °C (76%). The hydroxyl groups in unsaturated polyester resin have been reported to react with geopolymers to exclude water molecules via polycondensation and form a continuous gel when the geopolymers are heated until the thermolysis of the resin, thus improving their pore structures [58]. Further increasing the temperature to 900 °C may decompose the gel, thus leading to a greater flexural strength loss of specimen GC-1. Moreover, the porosity increased and the pores connected at elevated temperatures, therefore further reducing the strength [59].

As temperature increased from 300 to 900 $^{\circ}$ C, the mass loss ratio of GC-1 ranged from 6.4% to 21.0% and that of GC-0 ranged from 5.8% to 23.5%. The mass loss shows a sudden increase at 900 $^{\circ}$ C for both GC-0 and GC-1 specimens. The mass loss below 600 $^{\circ}$ C can be attributed to the evaporation of condensed hydroxyl groups and free water [29]. Further increasing the temperature resulted in the decomposition of unhydrated and hydrated compounds.

3.2.2. Microstructures

The SEM microstructures of specimen GC-1 after high-temperature exposure and compression are shown in Fig. 14. The failure surfaces of the samples exposed to 300 $^{\circ}\text{C}$ had needle-shaped gels, cracks, voids, and unreacted FA spheres. When the samples were heated to 600 $^{\circ}\text{C}$, they became more porous because the free water and hydroxyl groups inside the samples turned to vapor and were gradually released, thus causing flaws or cracks in geopolymers and reducing their mechanical properties [60]. Further increasing the temperature to 900 $^{\circ}\text{C}$ caused the porous structure to collapse, leading to a remarkable decrease of the mechanical properties.

The EDS results of specimen GC-1 after exposure to 300, 600, and 900 $^{\circ}$ C indicate that the Al/Si atomic ratios were 0.93, 0.72, and 0.68, respectively, the Na/Si atomic ratios were 0.11, 0.57, and 0.82, respectively, and the Ca/Si atomic ratios were 0.08, 0.10, and 0, respectively. The Al/Si ratios of samples at elevated temperatures were substantially higher than those of the samples at ambient temperature, which may indicate the deterioration of the poly-sialate-siloxo and poly-sialate-disiloxo matrix [61]. Higher concentrations of Si and Al compared with Ca indicate that N-A-S-H was the main geo-polymerization product, and that carbonate decomposed at high temperature.

4. Summary and conclusions

The following conclusions summarize the notable properties of GFRP powder/FA geopolymers and highlight their efficiency as a potential construction product.

- (1) Increasing the content of GFRP powder from 20 to 30 wt% had an insignificant effect on the setting time and flow value, whereas further increasing the GFRP powder content to 40 wt% led to a decrease in the setting time and flow value. Replacing low-calcium FA with GFRP powder can accelerate the geopolymerization process, thus shortening the setting time and reducing the flow value of geopolymer paste. The geopolymer concrete containing GFRP powder had a higher slump than the geopolymer concrete without GFRP powder, due to the low-absorbent nature of the GFRP powder.
- (2) Both of the optimum compressive and flexural strengths of geopolymer paste were obtained at 30 wt% GFRP powder content, an activator concentration of 85%, L/S of 0.65, and activator solution modulus of 1.3. Incorporating 30 wt% GFRP powder in geopolymer concrete to replace FA can increase the compressive and flexural strengths of geopolymer concrete by 28%. The GFRP powder/FA-based geopolymer concrete with s/a = 0.38 and a/b = 4.8 produced the highest compressive strength.
- (3) The color of the GFRP powder/FA-based geopolymer concrete changed when the temperature increased to 600 °C, and reticulate cracks occurred at 900 °C. Both the geopolymer concrete with and without GFRP powder showed a similar decreasing tendency of compressive and flexural strengths with increasing temperature. The mass loss showed a sudden increase at 900 °C for the geopolymer concrete with and without GFRP powder owing to the decomposition of unhydrated and hydrated compounds.
- (4) Microstructural analysis indicates that the main gel products of the GFRP powder/FA-based geopolymer concrete were N-A-S-H coexisting with C-S-H or C-A-S-H gels. A porous microstructure formed after exposure to 600 °C due to the evaporation of free water and hydroxyl groups, and then collapsed at 900 °C. The Al/ Si ratios of the samples exposed to elevated temperatures were substantially higher than those at ambient temperature, indicating the deterioration of the poly-sialate-siloxo and polysialate-disiloxo matrix.

Declaration of competing interest

The authors declare that they have no known competing financial interests or personal relationships that could have appeared to influence the work reported in this paper.

Acknowledgements

This study was financially supported by the National Natural Science Foundation of China (Grant 51578283), Top Six Talent Projects in Jiangsu Province, China (Grant No. JZ-024), and Science and Technology Projects in Jiangsu Construction System, China (Grant 2021ZD05).

References

- [1] H. Xie, H. Fang, W. Cai, L. Wan, R. Huo, D. Hui, Development of an innovative composite sandwich matting with GFRP facesheets and wood core, Rev. Adv. Mater. Sci. 60 (2021) 80–91, https://doi.org/10.1515/rams-2021-0016.
- [2] Z. Guo, Q. Zhu, W. Wu, Y.Y. Chen, Research on bond-slip performance between pultruded glass fiber-reinforced polymer tube and nano-CaCO₃ concrete, Nanotechnol. Rev. 9 (2020) 637–649, https://doi.org/10.1515/ntrev-2020-0036.
- [3] Z. Chen, J. Wang, J. Chen, H. GangaRao, R. Liang, W. Liu, Responses of concrete-filled FRP tubular and concrete-filled FRP-steel double skin tubular columns under horizontal impact, Thin, Wall. Struct. 155 (2020) 106941, https://doi.org/10.1016/j.tws.2020.106941
- [4] J. Chen, J. Wang, A. Ni, Recycling and reuse of composite materials for wind turbine blades: an overview, J. Reinforc. Plast. Compos. 38 (2019) 567–577, https://doi.org/10.1177/0731684419833470.
- [5] M. Rani, P. Choudhary, V. Krishnan, S. Zafar, A review on recycling and reuse methods for carbon fiber/glass fiber composites waste from wind turbine blades, Compos. B Eng. 215 (2021), https://doi.org/10.1016/j.compositesb.2021.108768, 108768.
- [6] M. Reuter, A. Van Schaik, Opportunities and limits of recycling: a dynamic-model-based analysis, MRS Bull. 37 (2012) 339–347, https://doi.org/10.1557/mrs.2012.57.
- [7] N. Ranjbar, C. Kuenzel, J. Spangenberg, M. Mehrali, Hardening evolution of geopolymers from setting to equilibrium: a review, Cement Concr. Compos. 114 (2020) 103729, https://doi.org/10.1016/j.cemconcomp.2020.103729.
- [8] P. Lemougna, K. Wang, Q. Tang, U. Melo, X. Cui, Recent developments on inorganic polymers synthesis and applications, Ceram. Int. 42 (2016) 15142–15159, https://doi.org/10.1016/j.ceramint.2016.07.027.
- [9] N. Shehataa, E.T.S. Alibc, M.A. Abdelkareembcd, Recent progress in environmentally friendly geopolymers: a review, Sci. Total Environ. 189 (2021) 143166, https://doi.org/10.1016/j.scitotenv.2020.143166.
- [10] H. Rashidian-Dezfouli, P.R. Rangaraju, V.S.K. Kothala, Influence of selected parameters on compressive strength of geopolymer produced from ground glass fiber, Construct. Build. Mater. 162 (2018) 393–405, https://doi.org/10.1016/j. conbuildmat.2017.09.166.
- [11] P. He, B. Zhang, J.X. Lu, S.P. Chi, A ternary optimization of alkali-activated cement mortars incorporating glass powder, slag and calcium aluminate cement, Construct. Build. Mater. 240 (2020) 117983, https://doi.org/10.1016/j. conbuildmat.2019.117983.
- [12] H. Rashidian-Dezfouli, P.R. Rangaraju, Comparison of strength and durability characteristics of a geopolymer produced from fly ash, ground glass fiber and glass powder, Mater. Construcción 67 (2017), https://doi.org/10.3989/mc.2017.05416.
- [13] H. Rashidian-Dezfouli, P.R. Rangaraju, Study on the effect of selected parameters on the alkali-silica reaction of aggregate in ground glass fiber and fly ash-based geopolymer mortars, Construct. Build. Mater. 271 (2021) 121549, https://doi.org/ 10.1016/j.conbuildmat.2020.121549.
- [14] H. Rashidian-Dezfouli, P.R. Rangaraju, A comparative study on the durability of geopolymers produced with ground glass fiber, fly ash, and glass-powder in sodium sulfate solution, Construct. Build. Mater. 153 (2017) 996–1009, https://doi.org/ 10.1016/j.conbuildmat.2017.07.139.
- [15] G. Taveri, E. Bernardo, I. Dlouhy, Mechanical performance of glass-based geopolymer matrix composites reinforced with cellulose fibers, Materials 11 (2018) 2395. https://doi.org/10.3390/ma11122395.
- [16] P. Manikandan, V. VasugilCa, A critical review of waste glass powder as an aluminosilicate source material for sustainable geopolymer concrete production, silicon, Net 13 (2021) 3649–3663, https://doi.org/10.1007/s12633-020-00929-w.
- [17] S. Dadsetan, H. Siad, M. Lachemi, M. Sahmaran, Extensive evaluation on the effect of glass powder on the rheology, strength, and microstructure of metakaolin-based geopolymer binders, Construct. Build. Mater. 268 (2021) 121168, https://doi.org/ 10.1016/j.conbuildmat.2020.121168.
- [18] R. Si, Q. Dai, S. Guo, J. Wang, Mechanical property, nanopore structure and drying shrinkage of metakaolin-based geopolymer with waste glass powder, J. Clean. Prod. 242 (2020) 118502, https://doi.org/10.1016/j.jclepro.2019.118502.
- [19] A.M. Amaro, M.I.M. Pinto, P.N.B. Reis, M.A. Neto, S.M.R. Lopes, Structural integrity of glass/epoxy composites embedded in cement or geopolymer mortars, Compos. Struct. 206 (2018) 509–516, https://doi.org/10.1016/j. compstruct.2018.08.060.
- [20] J. Ren, S. Guo, J. Su, T. Zhao, J. Chen, S. Zhang, A novel TiO₂/Epoxy resin composited geopolymer with great durability in wetting-drying and phosphoric

- acid solution, J. Clean. Prod. 227 (2019) 849–860, https://doi.org/10.1016/j.
- [21] C. Ferone, G. Roviello, F. Colangelo, R. Cioffi, O. Tarallo, Novel hybrid organic-geopolymer materials, Appl. Clay Sci. 73 (2013) 42–50, https://doi.org/10.1016/j.clay.2012.11.001.
- [22] A. Zhang, Effect of epoxy resin on mechanical properties of metakaolin based geopolymer and microscopic analysis, J. Wuhan Univ. Technol.-Materials Sci. Ed. 35 (2020) 431–434, https://doi.org/10.1007/s11595-020-2274-9.
- [23] S. Wang, X. Ma, L. He, Z. Zhang, L. Li, Y. Li, High strength inorganic-organic polymer composites (IOPC) manufactured by mold pressing of geopolymers, Construct. Build. Mater. 198 (2019) 501–511, https://doi.org/10.1016/j. conbuildmat.2018.11.281.
- [24] F. Colangelo, G. Roviello, L. Ricciotti, V. Ferrándiz-Mas, F. Messina, C. Ferone, O. Tarallo, R. Cioffi, C.R. Cheeseman, Mechanical and thermal properties of lightweight geopolymer composites, Cement Concr. Compos. 86 (2018) 266–272, https://doi.org/10.1016/j.cemconcomp.2017.11.016.
- [25] G. Roviello, L. Ricciotti, O. Tarallo, C. Ferone, F. Colangelo, V. Roviello, R. Cioffi, Innovative fly ash geopolymer-epoxy composites: preparation, microstructure and mechanical properties, Materials 9 (2016) 461, https://doi.org/10.3390/ prep60461
- [26] T. Lingyu, H. Dongpo, Z. Jianing, W. Hongguang, Durability of geopolymers and geopolymer concretes: a review, Rev. Adv. Mater. Sci. 60 (2021) 1–14, https://doi. org/10.1515/rams-2021-0002.
- [27] X. Jiang, R. Xiao, Y. Ma, M. Zhang, B. Huang, Influence of waste glass powder on the physico-mechanical properties and microstructures of fly ash-based geopolymer paste after exposure to high temperatures, Construct. Build. Mater. 262 (2020) 120579, https://doi.org/10.1016/j.conbuildmat.2020.120579.
- [28] M. Bazli, M. Abolfazli, Mechanical properties of fibre reinforced polymers under elevated temperatures: an overview, polymers, Baseline 12 (2020) E2600, https:// doi.org/10.3390/polym12112600.
- [29] G. Roviello, L. Ricciotti, C. Ferone, F. Colangelo, O. Tarallo, Fire resistant melamine based organic-geopolymer hybrid composites, Cement Concr. Compos. 59 (2015) 89–99, https://doi.org/10.1016/j.cemconcomp.2015.03.007.
- [30] Y. Zhang, S. Li, Y. Wang, D. Xu, Microstructural and strength evolutions of geopolymer composite reinforced by resin exposed to elevated temperature, J. Non-Cryst. Solids 358 (2012) 620–624, https://doi.org/10.1016/j. inoncrysol.2011.11.006.
- [31] J.C. Capricho, B. Fox, N. Hameed, Multifunctionality in epoxy resins, Polym. Rev. 60 (2020) 1-41, https://doi.org/10.1080/15583724.2019.1650063.
- [32] ASTM C618-19, Standard Specification for Coal Fly Ash and Raw or Calcined Natural Pozzolan for Use in Concrete, PA, USA, 2019.
- [33] O. Wan-En, L. Yun-Ming, H. Cheng-Yong, M.M.A.B. Abdullah, L.-Y. Li, L.N. Ho, F. K. Loong, O. Shee-Ween, N. Hui-Teng, N. Hui-Teng, N.A. Jaya, Comparative mechanical and microstructural properties of high calcium fly ash one-part geopolymers activated with Na₂SiO₃-anhydrous and NaAlO₂, J. Mater. Res. Technol. 15 (2021) 3850–3866, https://doi.org/10.1016/j.jmrt.2021.10.018.
- [34] C. Shi, Steel slag its production, processing, characteristics, and cementitious properties, J. Mater. Civ. Eng. 16 (2005) 230–236, https://doi.org/10.1061/ (ASCE)0899-1561(2004)16:3(230).
- [35] S. Hu, H. Wang, G. Zhang, Q. Ding, Bonding and abrasion resistance of geopolymeric repair material made with steel slag, Cement Concr. Compos. 30 (2008) 239–244, https://doi.org/10.1016/j.cemconcomp.2007.04.004.
- [36] C. Shi, D. Roy, Alkali-Activated Cements and Concretes, Crc Press, 2006.
- [37] X. Guo, X. Pan, Effects of steel slag on mechanical properties and mechanism of fly ash-based geopolymer, J. Mater. Civ. Eng. 32 (2020), 04019348, https://doi.org/ 10.1061/(asce)mt.1943-5533.0003012.
- [38] W. Huo, Z. Zhu, J. Zhang, Z. Kang, S. Pu, Y. Wan, Utilization of OPC and FA to enhance reclaimed lime-fly ash macadam based geopolymers cured at ambient temperature, Construct. Build. Mater. 303 (2021) 124378, https://doi.org/ 10.1016/i.conbuildmat.2021.124378.
- [39] P. Nuaklong, V. Sata, P. Chindaprasirt, Influence of recycled aggregate on fly ash geopolymer concrete properties, J. Clean. Prod. 112 (2016) 2300–2307, https:// doi.org/10.1016/j.jclepro.2015.10.109.
- [40] W. Zhou, C. Yan, P. Duan, Y. Liu, Z. Zhang, X. Qiu, D. Li, A comparative study of high- and low-Al₂O₃ fly ash based-geopolymers: the role of mix proportion factors and curing temperature, Mater. Des. 95 (2016) 63–74, https://doi.org/10.1016/j. matdes.2016.01.084.

- [41] P. Nath, P. Sarker, Effect of GGBFS on setting, workability and early strength properties of fly ash geopolymer concrete cured in ambient condition, Construct. Build. Mater. 66 (2014) 163–171, https://doi.org/10.1016/j. conbuildmat.2014.05.080.
- [42] GB/T 1346-2011, Test Method for Water Requirement of Normal Consistency, Setting Time and Soundness of the Portland Cement, National Standards of People's Republic of China, China, 2011.
- [43] GB/T 8077-2012, Method for Testing Uniformity of Concrete Admixture, National Standards of People's Republic of China, China, 2012.
- [44] GB/T 50080-2016, Standard for Test Method of Performance on Ordinary Fresh Concrete, National Standards of People's Republic of China, China, 2016.
- [45] GB/T 17671-1999, Method of Testing Cements-Determination of Strength, National Standards of People's Republic of China, China, 1999.
- [46] GB/T50081-2019, Standard for Test Methods of Concrete Physical and Mechanical Properties, National Standards of People's Republic of China, China, 2019.
- [47] P. Nath, P.K. Sarker, Use of OPC to improve setting and early strength properties of low calcium fly ash geopolymer concrete cured at room temperature, Cement Concr. Compos. 55 (2015) 205–214, https://doi.org/10.1016/j. cemprocump. 2014.08.008
- [48] P. Chindaprasirt, P. De Silva, K. Sagoe-Crentsil, S. Hanjitsuwan, Effect of SiO₂ and Al₂O₃ on the setting and hardening of high calcium fly ash-based geopolymer systems, J. Mater. Sci. 47 (2012) 4876–4883, https://doi.org/10.1007/s10853-012-6353-y.
- [49] U. Rattanasak, K. Pankhet, P. Chindaprasirt, Effect of chemical admixtures on properties of high-calcium fly ash geopolymer, Int. J. Min. Met. Mater. 18 (2011) 364–369, https://doi.org/10.1007/S12613-011-0448-3.
- [50] M.N.S. Hadi, H. Zhang, S. Parkinson, Optimum mix design of geopolymer pastes and concretes cured in ambient condition based on compressive strength, setting time and workability, J. Build. Eng. 23 (2019) 301–313, https://doi.org/10.1016/ j.jobe.2019.02.006.
- [51] M.A.M. Ariffin, M.W. Hussin, M.A.R. Bhutta, Mix design and compressive strength of geopolymer concrete containing blended ash from agro-industrial wastes, Adv. Mater. Res. 339 (2011) 452–457. https://doi.org/10.4028/www.scientific.net/AM R.339.452.
- [52] W. Song, Z. Zhu, Y. Peng, Y. Wan, X. Xu, S. Pu, S. Song, Y. Wei, Effect of steel slag on fresh, hardened and microstructural properties of high-calcium fly ash based geopolymers at standard curing condition, Construct. Build. Mater. 229 (2019) 116933, https://doi.org/10.1016/j.conbuildmat.2019.116933.
- [53] X. Guo, X. Pan, Effects of steel slag on mechanical properties and mechanism of fly ash-based geopolymer, J. Mater. Civ. Eng. 32 (2020), https://doi.org/10.1061/ (ASCEMT.1943-5533.0003012.
- [54] Y. Ding, T. Cheng, Y. Dai, Application of geopolymer paste for concrete repair, Struct. Concr. 18 (2017) 561–570, https://doi.org/10.1002/suco.201600161.
- [55] A.S. Albidah, M. Alghannam, H. Abbas, T.H. Almusallam, Y.A. Al-Salloum, Characteristics of metakaolin-based geopolymer concrete for different mix design parameters, J. Mater. Res. Technol. 10 (2021) 84–98, https://doi.org/10.1016/j. jmrt.2020.11.104.
- [56] H. Sethi, P.P. Bansal, R. Sharma, Effect of addition of GGBS and glass powder on the properties of geopolymer concrete, Ijst-T. Civ. Eng. 43 (2019) 607–617, https://doi.org/10.1007/s40996-018-0202-4.
- [57] M.S. Reddy, P. Dinakar, B.H. Rao, Mix design development of fly ash and ground granulated blast furnace slag based geopolymer concrete, J. Build. Eng. 20 (2018) 712–722, https://doi.org/10.1016/j.jobe.2018.09.010.
- [58] Z. Pan, Z. Tao, T. Murphy, R. Wuhrer, High temperature performance of mortars containing fine glass powders, J. Clean. Prod. 162 (2017) 16–26, https://doi.org/ 10.1016/j.jclepro.2017.06.003.
- [59] P. He, D. Jia, T. Lin, M. Wang, Y. Zhou, Effects of high-temperature heat treatment on the mechanical properties of unidirectional carbon fiber reinforced geopolymer composites, Ceram. Int. 36 (2010) 1447–1453, https://doi.org/10.1016/j. ceramint.2010.02.012.
- [60] H. Song, L. Wei, Y. Ji, L. Cao, F. Cheng, Heavy metal fixing and heat resistance abilities of coal fly ash-waste glass based geopolymers by hydrothermal hot pressing, Adv. Powder Technol. 29 (2018) 1487–1492, https://doi.org/10.1016/j. apt.2018.03.013.
- [61] P.D. Silva, K. Sagoe-Crenstil, V. Sirivivatnanon, Kinetics of geopolymerization: role of Al₂O₃ and SiO₂, Cement Concr. Res. 37 (2007) 512–518, https://doi.org/ 10.1016/j.cemconres.2007.01.003.